PLASMA PHYSICS AND PLASMA METHODS

UDC 533.9; 534-16
EDN: VGCLXD

PACS: 52.75Fk; 41.75Fr; 41.75Ht; 62.50Ef

Evaluation of the influence of plasma processes in the vacuum diode of Kalmar high-current electron accelerator on the development of shock-wave processes in targets

© E. D. Kazakov[1,2,3,4,*], M. Yu. Orlov[1], A. R. Smirnova[1,3,4], M. G. Strizhakov[1], K. A. Sunchugashev[1],L. M. Yusupova[1,2], S. I. Tkachenko[1,3,4,5]

[1] *National Research Center Kurchatov Institute, Moscow, 123182 Russia*
[*] *E-mail: kazakov_ed@nrcki.ru*
[2] *MPEI National Research Institute, Moscow, 111250 Russia*
[3] *Moscow Institute of Physics and Technology (National Research University), Dolgoprudny, Moscow Region, 141701 Russia*
[4] *Keldysh Institute of Applied Mathematics of the Russian Academy of Science, Moscow, 125047 Russia*
[5] *Joint Institute for High Temperatures of the Russian Academy of Sciences, Moscow, 125412*

Received 11.11.2024; revised 13.01.2025; accepted 14.02.2025
Scientific specialty code: 1.3.9

The influence of diode plasma on the formation and propagation of compression and shock waves inside targets is considered as part of studying the impact of high-current electron beams on solid targets. Experimental studies were carried out on the Kalmar installation generating a high-current electron beam. For the purpose of evaluation, numerical modeling of processes occurring in the plasma-filled diode in terms of one-dimensional magnetohydrodynamics (MHD) was carried out. The modeling results confirm that plasma can provide the pressure sufficient to create the secondary compression waves observed during the experiment.

Keywords: diode plasma; high-current electron beam; transparent targets; shock-wave processes.

DOI: 10.51368/1996-0948-2025-2-55-61

Introduction

Studying the formation and propagation of shock waves inside various materials under powerful pulse impacts is of relevance, since the growing number of new composite and polymeric materials are finding use in aviation, rocket and space technology, shipbuilding and special applications [1]. Experimental research in this area has been conducted for over fifty years using various types of impact on samples [2–6]. The main instruments initiating the mechanical shock wave impact are ballistic and explosive generators [7] and electroexplosive devices [8]. Along with them, high-power pulsed lasers, magnetic-pulse generators [9], as well as high-current electron and ion accelerators are actively used. This paper describes the features of shock-wave processes occurring in transparent materials impacted by a high-current electron beam generated by Kalmar installation (current up to 35 kA, diode voltage up to 350 kV, electron beam duration ≈ 100 ns).

Relatively high penetration power is among the specific features of such electron beams as a source of shock waves. Since the duration of beam action is about one hundred nanoseconds, the energy is released in the surface layer of not more than several hundred micrometers in thickness (up to 80 % of electrons are absorbed in the layer less than 100 microns thick), and the release time of such region is at least 500 ns, so the process of beam energy absorption can be considered isochoric. In most studies, various parameters on the target surface are evaluated considering only the interaction of the electron beam with the target surface and release of the energy absorption region. However, after the electron beam has passed, plasma is formed in the diode gap [10], the influence of which is usually neglected. Some experimental results demonstrating the dynamics of shock wave passing through the target [10, 11] give reason for considering the influence of diode plasma on the formation and propagation of shock waves inside the target in more details.

The issue of influence of diode plasma on the formation and propagation of compression and shock waves inside targets was brought up earlier during study of the impact of high-current electron beams on condensed targets. However, so far there are no findings that confirm or refute this. As a result of modeling the anode flame [12], quite extreme plasma parameters were obtained (average electron temperature $T_e \approx 10$ eV, average concentration $n_e > 5\times10^{17}$ cm^{-3}). One-dimensional MHD modeling of the plasma column parameters that we undertook confirms the assumption that the plasma pressure can reach values sufficient to give rise to compression waves, which can be observed during experiments.

Experimental research

Experiments to study the influence of diode plasma on the formation and movement of shock and compression waves in transparent targets were carried out using Kalmar high-current accelerator [13]. Target samples made of various transparent materials were attached to the anode assembly plate. The residual pressure in the vacuum chamber was not more than 10^{-2} Pa.

The optical diagnostic system is based on probing the diode gap and/or target with laser radiation perpendicularly to the diode axis. Laser radiation passes via the diagnostic windows through the area under study. The image is transferred to the photocathode of SFER-6 electron-optical camera operating in streak image mode by means of the system of lenses and mirrors [9]. Since the typical durations of plasma and shock-wave processes differ by approximately an order of magnitude, plasma processes can be identified quantitatively only on streak image with. It should be noted that plasma parameters in the anode region can take on values at which plasma cannot be identified with existing diagnostics.

Figure 1 shows the combined streak image recorded by the shadow photography method while simultaneously recording the plasma's own glow. One can see the shadow appearing against the background of the probing radiation in the upper part of the image. This shadow appears when the refractive index changes as the compression or shock wave passes in a target attached to the rear surface of the anode plate. In the lower part of the image (below the time axis), the plasma's own glow in the accelerator diode can be observed. The probing radiation did not pass through the diode gap since it was blocked by the screen.

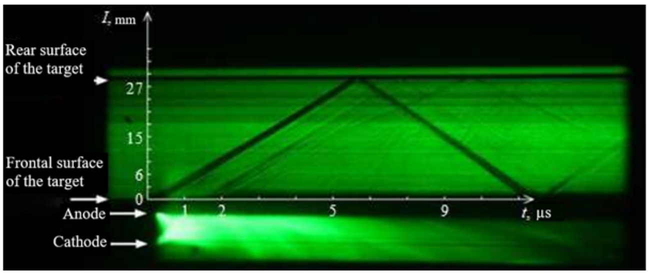

Fig. 1. The combined streak image recorded by the shadow photography method while simultaneously recording the plasma's own glow. The time-analyzing slit is oriented along the beam axis. The energy of the electron beam in the shot was 450 J; the target was made of glass (LK-5)

As can be seen from streak image, during the first 300–400 ns a shock wave is formed, the propagation speed of which is ~5.4 km/s. One can see in the lower part of the streak image that, by the end of this time interval, the bright own glow spreading from the electrodes to the center covers the diode gap. It can be concluded that the radiating plasma fills up the diode gap. By the time equaling to 1.5–2 µs the plasma's own glow becomes less intense. After ~2 µs, multiple darkenings appear within the target volume, each may correspond to the propagation of compression waves in the material. Occurrence of these waves at the late stages of anode plasma expansion may be caused by the excessive pressure in the anode region arising in the plasma channel.

The current and voltage in the diode gap were measured using a shunt and a capacitive divider, respectively [14]. With the current and voltage known, one can determine the power and integral energy input by the beam to the sample.

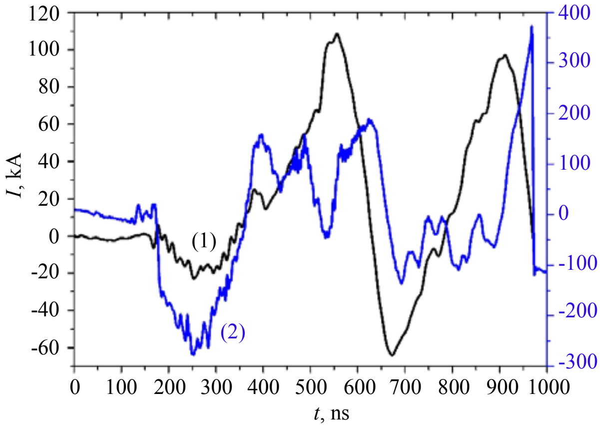

Fig. 2. The time dependences of the current (1) and voltage (2) measured at the diode gap

Figure 2 shows the characteristic time dependence of the electron beam current and conduction current through the diode. The electron beam can be seen to be formed in the diode in the time interval from 150 ns to 350 ns; after which the diode gap is filled with plasma, which initiates the current reversal at ~400 ns. After the diode is closed by plasma, the alternating current can be observed, with its amplitude decreasing. The diode is closed due to its filling with plasma flows from the cathode and anode. Plasma appearing at the cathode is caused by the surface explosion (explosive emission), and the one appearing at the anode is caused by the interaction of a beam of high-energy electrons with the target surface. The presence of current in the diode gap means that the plasma closing the diode has high conductivity.

Mathematical modeling

To determine the range of parameters at which diode plasma influences the generation of shock waves inside the target, a problem to model the processes occurring in the cylindrical plasma channel with current was formulated. The plasma channel formation stage was not considered. This problem was solved in terms of one-dimensional (coordinate r is directed parallel to the target surface; the origin of coordinates is located at the point corresponding to the electron beam axis) single-temperature magnetohydrodynamics (MHD) in the cylindrical coordinate system. The system of MHD equations using Lanrange variables is written below:

$$\frac{dm}{dt} = 0, \quad (1)$$

$$\rho \frac{dv}{dt} = -\frac{\partial P}{\partial r} - \frac{1}{2\mu_0 r^2} \cdot \frac{\partial \left(r^2 B_\varphi^{\ 2} \right)}{\partial r}, \quad (2)$$

$$\rho \frac{d\varepsilon}{dt} = -P \frac{\partial (rv)}{\partial r} + \frac{j^2}{\sigma}, \quad (3)$$

$$\frac{d\left(\mu B_\varphi \right)}{dt} = \frac{\partial}{\partial r} \left[\frac{1}{\sigma r} \cdot \frac{\partial \left(r B_\varphi \right)}{\partial r} \right], \quad (4)$$

where m is the mass; $\rho = m_c n$ is the density; m_c is the carbon atom mass; v is the velocity; P is the flow pressure; μ is the permeability; B_φ is the magnetic field induction; $j = \frac{1}{\mu_0 r} \frac{\partial \left(r B_\varphi \right)}{\partial r}$ is the current density; σ is the conductivity; T is the temperature; n is the concentration. To describe the thermodynamic properties of the medium, the ideal plasma model and the Spitzer conductivity model were used. Initial and boundary conditions for the described problem were written using the results obtained from processing the experimental data: maximum plasma concentration at the initial moment was equal to $n_0 = 10^{17}$ cm^{-3}, initial radius of the cylindrical plasma column was equal to $r_0 = 1$ cm, initial plasma temperature was equal to $T_0 = 10$ eV, magnetic field induction at the outer boundary (r_{out}) of plasma channel $B_\varphi(r_{out},t) = \mu_0 I(t)/\{2\pi\ r_{out}(t)\}$; the magnetic field and velocity field at the initial moment were set to zero. The model considered the singly-ionized plasma; the initial distribution of plasma concentration depending on the radius is cosine. The total current value was determined by sinusoidal dependence $I(t) = I_{max} \sin(\omega t)$, $\omega = (2\pi/400)$ ns^{-1}.

Figure 3 shows the radial dependence of the pressure in the plasma column obtained by the numerical simulation with I_{max} = 100 kA.

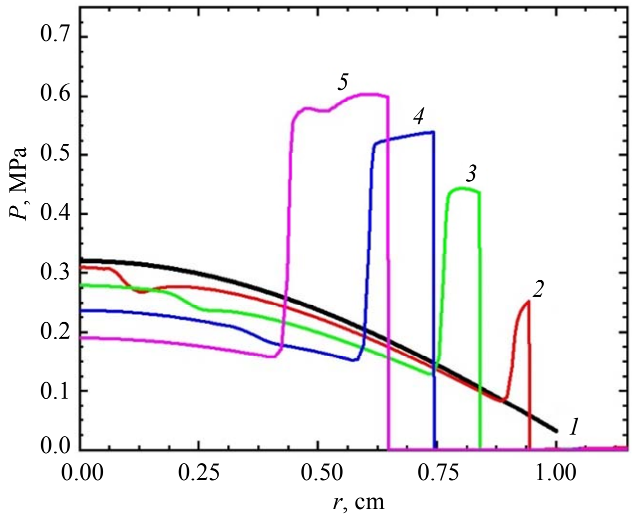

Fig. 3. The radial dependence of the pressure in the plasma column. The numbers indicate the time counted from the start of the conduction current (equal to 400 ns in Fig. 2): 1 – 0 ns, 2 – 100 ns, 3 – 200 ns, 4 – 300 ns, 5 – 400 ns

As Figure 3 shows, the pressure increases near the outer surface of the plasma cylindrical sheath, and the region of the increased pressure shifts toward the axis of symmetry over time. This is due to the magnetic pressure pressing the low-density peripheral plasma toward the axis while the gas-dynamic pressure is simultaneously pushing the high-density substance away from the axis, thus forming a region with the increased density and consequently, with the increased pressure at the plasma region periphery.

Discussion of the results

When the electron beam interacts with the target surface, the torch of anode plasma is formed, and when high-power currents pass through the electrodes, plasma flow formed by explosive electron emission is separated from the cathode. At a certain moment, these two flows overlap the diode (see the lower part of the streak image in Fig. 1, which shows the plasma's own glow in the accelerator diode), thus forming the conductance channel in the diode for the current passing after the pulse of the subrelativistic electron beam, i.e. after 400 ns as shown in Fig. 2.

Figure 4 shows a transverse streak image: a image of the central part of the diode gap perpendicular to the diode axis is sweeped in time. As can be seen in Figure 4, the anode plasma reaches the recording region by the ~300th nanosecond; then, within ~100 ns, the diode gap is filled with almost uniform plasma, the transverse dimension of which increases from 0.5 cm to~ 1 cm by 400 ns, i.e., the radial velocity at the outer boundary being observed is equal to ~ 3×10^4 m/s. After the time moment corresponding to 440 ns, the radiating plasma can be observed to be pressed along its outer visible boundary; in the same region (its thickness being ~1 mm), the plasma's own glow is more intense. According to the modeling results (Fig. 3), at the time corresponding to 200–300 ns from the conduction current start in the plasma channel a pressing region of the same size and with the same pressing rate of ~ 10^4 m/s is formed; the pressure in this region is higher than in other parts of the plasma. Increase of the plasma pressure will lead to the increased pressure at the plasma column ends, which can give rise to another compression or shock waves that are not directly related to the impact of the electron beam on the target surface. Thus, considering the processes occurring in the diode plasma can have a significant impact on the study of the dynamics of the formation and passage of compression and shock waves in solid targets.

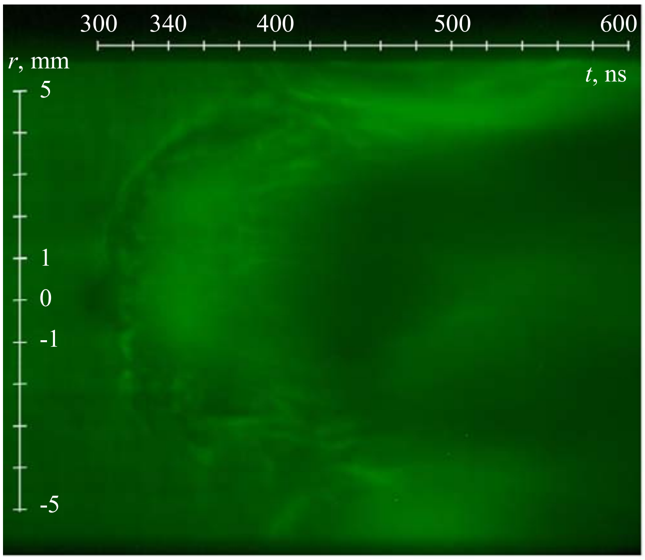

Fig. 4. The streak image recorded by the shadow photography method while simultaneously recording the plasma's own glow. The time-analyzing slit is oriented across the beam axis. The electron beam energy in the shot was 460 J

It is also worth noting that, as is shown in Fig. 1, some of these waves seem to change their propagation speed – they correspond to darkenings, the slope of which changes over time. The reason for the slope to change could be the process of wave formation not in the target surface region that corresponds to the beam axis, but, for example, near the outer boundary of the region where the beam and target interact. In this case compression waves will arrive at the region lying on the beam axis extension with different time delays, depending on the coordinate along the thickness of the target, which will cause the shadow with a slope changing along the target thickness.

Conclusion

Thus, both the experimental data and modeling results obtained in terms of one-dimensional magnetohydrodynamics confirm that the processes occurring in the diode plasma should be taken into account when studying the dynamics of formation and propagation of compression and shock waves in targets. Moreover, considering that plasma parameters in the diode gap are quite extreme, the plasma can also significantly impact the degree of surface destruction of the materials being tested. To advance the research described herein, the more detailed analysis of the experimental data is suggested, including using the modeling results that we plan to obtain from the improved model.

Mathematical modeling was carried out with the support of the Russian Science Foundation (project No. 23-21-00248).
Experiments using Kalmar installation were conducted as part of the state assignment from the National Research Center Kurchatov Institute.

REFERENCES

1. Kovalenko V. A. and Kondratyev A. V., Aviation and space equipment and technology, No. 5, 14–20 (2011) [in Russian].

2. Rudakov L. I., Babykin M. V., Gordeev A. V. et al. Generation and focusing of high-current relativistic electron beams. Moscow, Energoatomizdat, 1990 [in Russian].

3. Grabovsky E. V., Vorobyov O. Yu., Dyabilin K. S., Lebedev M. E., Ostrik A. V., Smirnov V. P. and Fortov V. E., JETP Letters **60** (1), 1–4 (1984).

4. Lomov S. A. Introduction to the General Theory of Singular Perturbations. Moscow, Nauka, 1981.

5. Kanel' G., Fortov V and Razorenov S., Physics-Uspekhi **50** (8), 771–791 (2007).

6. Didenko A. N., Ligachev A. E. and Kurakin I. B. Effect of charged particle beams on the surfaces of metals and alloys. Moscow, Energoatomizdat, 1987 [in Russian].

7. Kanel G. I., Razorenov S. V., Utkin A. V. and Fortov V. E. Shock-wave phenomena in condensed media. Moscow, “Yanus-K”, 1996 [in Russian].

8. Ryabinin Yu. N., Technical Physics, No. 26, 2661 (1956).

9. Krivosheev S. I., Technical Physics **50** (3), 334–340 (2005).

10. Demidov B. A., Kazakov E. D., Kalinin Yu. G. et al., Instruments and Experimental Techniques, **63**, 370–374 (2020).

11. Demidov B. A., Kazakov E. D., Kalinin Yu. G. et al., Applied Physics, No. 6, 74–78 (2018) [in Russian].

12. Ananyev S. S., Bagdasarov G. A., Gasilov V. A. et al., Plasma Physics Reports **43**, 726–732 (2017).

13. Demidov B. A., Ivkin M. V., Petrov V. A. and Fanchenko S. D., Atomic Energy **46** (2), 111–116 (1979).

14. Kazakov E. D. et al., Plasma Physics Reports **47**, 803–813 (2021).

About authors

Evgeny Davidovich Kazakov, Deputy Head of the Department, Candidate of Physics and Mathematics, National Research Center Kurchatov Institute (123182, Russia, Moscow, Academician Kurchatov Square, 1). MPEI National Research Institute (111250, Russia, Moscow, Krasnokazarmennaya Ulitsa, 14). Moscow Institute of Physics and Technology (National Research University) (141701, Russia, Moscow Region, Dolgoprudny, Institutsky Per., 9). Keldysh Institute of Applied Mathematics of the Russian Academy of Science (125047, Russia, Moscow, Miusskaya, 4). E-mail: kazakov_ed@nrcki.ru SPIN code 2936-1306, Author ID 184827

Mikhail Yurievich Orlov, Research Engineer, National Research Center Kurchatov Institute (123182, Russia, Moscow, Academician Kurchatov Square, 1). E-mail: mosgotron@gmail.com

Anna Romanovna Smirnova, Junior Research Assistant, graduate student, National Research Center Kurchatov Institute (123182, Russia, Moscow, Academician Kurchatov Square, 1). Moscow Institute of Physics and Technology (National Research University) (141701, Russia, Moscow Region, Dolgoprudny, Institutsky Per., 9). Keldysh Institute of Applied Mathematics of the Russian Academy of Science (125047, Russia, Moscow, Miusskaya, 4). E-mail: anya4113@gmail.com SPIN code 8607-4923, Author ID 1254979

Mikhail Gennadievich Strizhakov, Research Assistant, National Research Center Kurchatov Institute (123182, Russia, Moscow, Academician Kurchatov Square, 1). E-mail: strizhakov_mg@nrcki.ru SPIN code 1430-1600, Author ID: 824117

Kirill Alexandrovich Sunchugashev, Laboratory Assistant, National Research Center Kurchatov Institute (123182, Russia, Moscow, Academician Kurchatov Square, 1). E-mail: 1032182603@pfur.ru

Liliya Maratovna Yusupova, Laboratory Assistant, student, National Research Center Kurchatov Institute (123182, Russia, Moscow, Academician Kurchatov Square, 1). MPEI National Research Institute (111250, Russia, Moscow, Krasnokazarmennaya Ulitsa, 14). E-mail: yusupova_lilia_m@mail.ru

Svetlana Ivanovna Tkachenko, Professor, Doctor of Physics and Mathematics Science, National Research Center Kurchatov Institute (123182, Russia, Moscow, Academician Kurchatov Square, 1). Moscow Institute of Physics and Technology (National Research University) (141701, Russia, Moscow Region, Dolgoprudny, Institutsky Per., 9). Keldysh Institute of Applied Mathematics of the Russian Academy of Science (125047, Russia, Moscow, Miusskaya, 4). United Institute of High Temperatures of the Russian Academy of Science (125412, Russia, Moscow, Izhorskaya Ulitsa, 13, bld. 2). E-mail: tkachenko@phystech.edu SPIN code 8352-8420, Author ID 108014